Journal of Applied Physics

Spatially focused microwave ignition of metallized energetic materials

Cite as: J. Appl. Phys. **127**, 055901 (2020); https://doi.org/10.1063/1.5134089
Submitted: 01 November 2019 . Accepted: 12 January 2020 . Published Online: 03 February 2020

Dylan J. Kline, Miles C. Rehwoldt, Charles J. Turner, Prithwish Biswas, George W. Mulholland, Shannon M. McDonnell, and Michael R. Zachariah

Journal of Applied Physics ARTICLE scitation.org/journal/jap

Spatially focused microwave ignition of metallized energetic materials

Cite as: J. Appl. Phys. **127**, 055901 (2020); doi: 10.1063/1.5134089
Submitted: 1 November 2019 · Accepted: 12 January 2020 ·
Published Online: 3 February 2020

Dylan J. Kline,[1,2] Miles C. Rehwoldt,[1,2] Charles J. Turner,[3] Prithwish Biswas,[1] George W. Mulholland,[2] Shannon M. McDonnell,[4] and Michael R. Zachariah[1,a)]

AFFILIATIONS

[1]Department of Chemical and Environmental Engineering, University of California, Riverside, California 92521, USA
[2]Department of Chemical and Biomolecular Engineering, University of Maryland, College Park, Maryland 20740, USA
[3]Department of Electrical and Computer Engineering, University of Maryland, College Park, Maryland 20740, USA
[4]Department of Chemistry and Biochemistry, University of Maryland, College Park, Maryland 20740, USA

[a)]**Author to whom correspondence should be addressed:** mrz@engr.ucr.edu

ABSTRACT

This study investigates the ability to locally ignite metallized propellants via microwave absorption. Metallized energetic composite films incorporating high mass loadings of aluminum and titanium nanoparticle fuels within a polyvinylidene fluoride (PVDF) polymer matrix were constructed by direct-write additive manufacturing (3D printing). Simulations of power absorption for both Ti and Al nanoparticles reveal that the passivating shell composition likely plays a significant role in the observed ignition phenomenon. Various architectures of interest were constructed for predictable microwave ignition and propellant propagation. It was found that, although aluminum nanoparticles and composites do not ignite via exposure to microwaves, titanium nanoparticles can be used as efficient reactive microwave susceptors enabling a localized ignition source. This approach enables various architectures of previously studied high energy Al/PVDF systems to be fabricated and outfitted with a microwave-sensitive titanium composite in strategic locations as a means of remote ignition for aluminum systems.

I. INTRODUCTION

Nanoenergetic materials are a class of exothermic heterogeneous solid mixtures with common applications in propellants, ignitors, and pyrotechnics. Nanoenergetics seek to enhance reactivity by incorporating nanoscale metallic particles for reduced diffusion length scale between fuel and oxidizer of high combustion enthalpy redox reactions. Although aluminum nanoparticles are the most commonly used nanometal in energetic research studies due to their high reaction enthalpy per gram and low cost, other energetic nanoscale metals such as tantalum[1] and titanium[2] have also been researched in past studies for their niche physical and chemical properties aside from their theoretical reaction enthalpy. Energetic formulations for propellant applications commonly integrate nanopowder within a polymer binder, which itself may also act as either a fuel, as in the case of traditionally used hydroxyl-terminated polybutadiene (HTPB),[3] or an oxidizer, as in the case of fluorinated polymer binders such as polyvinylidene fluoride (PVDF)[4] or Viton.[5] Recent research utilizing metallic formulations of this type have favored a variety of additive manufacturing techniques such as layer-by-layer deposition[6] and stereolithography[7] over traditional casting methods for the prospect of fast prototyping of highly customizable architectures with tunable parameters.[8]

Coupled with efforts for enhanced customization of 3D printed propellants, research has been devoted to probing the ability to throttle both combustion and ignition behavior of propellants remotely by irradiating energetic materials with microwave energy (MW energy).[9,10] Microwave radiation is defined by the frequency range of 300 MHz–300 GHz and is utilized under low power (~1 mW) for communications and relatively higher power (~1 kW) for dielectric heating of foods.

While the use of microwaves for heating has seen some success in applications for powder ceramic sintering,[11,12] synthesis of materials,[13–15] and demonstrating the initiation of crystalline high explosive monopropellant materials, such as 1,3,5-Trinitro-1,3,5-triazinane (RDX),[16] microwave heating of

metals and metal composites has had limited utility. The relatively high electrical conductivity of metals results in optically dense materials with skin depths of a few micrometers at conventional microwave oven frequencies (2.45 GHz). This means that most of the electromagnetic (EM) radiation is reflected at the material surface.[17,18] Modeling and experimental studies of metal powders demonstrated that a remedy for this problem is to use metallic powders that couple strongly with the magnetic field, as well as having particle diameters that are of the same order of magnitude as the skin depth for that material.[19–21] Particles that are too large will only heat at the surface, while particles much smaller than the skin depth will absorb only a fraction of the transmitted radiation in the form of heat generated by induced eddy currents as a result of the oscillating magnetic field.[19–21] As such, many experimental studies focusing on heating often utilize micrometer size powders that may also contain magnetic materials such as iron, cobalt, or nickel.[13,21–23]

Although sintering of powders of magnetic metals as a result of microwave heating to high temperatures has been realized, these magnetic materials have poor energetic performance and often take several minutes (10–30 min) to sinter.[12,13] Additionally, the enhancement of microwave absorption of size optimized aluminum particles (~3–4 μm) showed that the temperature to which the aluminum powder reaches from microwave irradiation is not enough to ignite the sample.[19] A follow-on study by Crane *et al.* looking at microwave heating of aluminum–iron oxide thermites demonstrated that the addition of microwave susceptors at ~10 weight percent (wt. %), in the form of carbon-based materials, will enhance heating by microwave irradiation.[24–26] However, this same study concluded that, while there was an enhancement of maximum temperature reached, the maximum reach of heating still fell short of the ignition threshold while also hindering reactivity and flame propagation speeds. Meir and Jerby have been successful at igniting micrometer sized aluminum–iron(II,III) oxide (magnetite) thermites within several seconds using a low power (~100 W), localized solid-state microwave-drill for enhanced microwave coupling and confined heating.[23] This approach has shown to be successful for this specific system; however, it is unclear whether this method will work for nanoscale systems with oxidizers that may not be magnetically sensitive.

Our study investigates the ability to rapidly initiate energetically relevant metallized nanoscale compositions via efficient microwave coupling, while maintaining a high overall energy density, reactivity, and combustion performance. Our preliminary microwave heating tests of prospective fuels in air showed that both micropowder and nanopowder aluminum did not demonstrate thermal ignition as a result of microwave heating. However, nanopowder titanium did demonstrate thermal ignition despite the aforementioned difficulties of using nanoscale nonmagnetic metals in microwave heating.[20,21] As a result of this initial finding, this study analyzes this behavior more in depth and employs the use of additive manufacturing techniques in order to design composition architectures that retrofit previously studied propellants with microwave-sensitive nanoscale titanium compositions to realize spatially localized microwave-ignitable propellants. This work also sets the stage for the fabrication of tailorable composite propellants that can be precisely and remotely ignited or staged by excitation of microwave-sensitive regions.

II. METHODS/EXPERIMENTAL

A. Mie theory calculations

Calculations of the absorbed microwave intensity by an ensemble of metal nanoparticles were modeled using the Mie theory, which considered both bare metal spherical nanoparticles and metal nanoparticles with an oxide shell. It has been assumed that the microwave needle antenna uniformly irradiates a circular area of 25 μm diameter on the sample surface with electromagnetic power deliverance of 15 W at a frequency of 2.45 GHz (discussed in Sec. II E). The absorption cross section, σ_A, for the bare metal particles and the coated metal particles is computed using BHMIE and BHCOAT subroutines, respectively.[27] Due to the lack of studies regarding core–shell nanoparticle microwave absorption, a more detailed study of the mechanism of microwave absorption of core–shell systems has been performed in tandem with this article by Biswas *et al.*, which has been generalized for a wider variety of materials.[28] The findings of this work, with respect to microwave heating of core–shell nanoparticles, are applied to our materials in question and discussed in Sec. III A.

B. Materials

Candidate materials studied in this project were determined based on three criteria: (1) high energy density nanoparticles, (2) the ability to act as an effective fuel for combustion, and (3) commercial availability with respect to cost. To meet the demands for high energy density, metallic nanoparticles were of primary interest due to their significant transient energy release during oxidation in comparison to other potential fuels (such as carbon). In particular, aluminum and titanium were metal fuels of primary consideration for reasons that are discussed in Sec. III A.

Aluminum nanoparticle powder (nAl) (~80 nm diameter and ~80% active by mass) [Fig. S1(a) in the supplementary material] used in this study was purchased from Novacentrix, and titanium nanoparticle powder (nTi) (30–50 nm diameter and ~70% active by mass) was purchased from U.S. Research Materials, Inc. [Fig. S1(b) in the supplementary material]. Nanometals were used as received with the active content (unoxidized metal content) of the nanoparticle core–shell structure determined using thermogravimetric analysis (TGA) from previous studies.[2,29] Two different sizes of micrometer aluminum powder, 3–4.5 μm [Fig. S2(a) in the supplementary material] and 10–14 μm [Fig. S2(b) in the supplementary material] in diameter, were purchased from Alfa Aesar and tested as received for preliminarily microwave absorption experiments. Poly(vinylidene fluoride) powder (PVDF, molecular weight = 534 000 g/mol) was purchased from Sigma Aldrich (Millipore Sigma), and *N*, *N*-dimethylformamide (DMF 99.8%) solvent was purchased from BDH chemicals. All chemicals were used as received.

C. Film fabrication

Energetic composites were fabricated using a System 30M pressure-driven 3D printer purchased from Hyrel 3D. An energetic precursor is utilized as a 3D printable ink in a direct-write, layer-by-layer additive manufacturing approach to create customized multicomposite architectures with distinct ignition and propagation

TABLE I. Energetic precursor formulations.

Fuel type (wt. %)	PVDF (wt. %)	Equivalence ratio (Φ)
Al: 25	75	1
Al: 65	35	5.3
Ti: 35	65	1
Ti: 50	50	1.9
Ti: 65	35	3.5

zones along the structure of the propellant. Each precursor 3D printable ink considered was formulated by dissolving a constant 70 mg/ml PVDF in DMF and adding various mass loadings of metal content in a similar way to past studies of such materials.[5,30]

Individual mixtures and particle loadings are listed in Table I where the specific loadings of fuel and oxidizer are formulated with various equivalence ratios, Φ, for one or more of the following reasons: stoichiometric conditions[29] for maximized energy output, ease of printability, enhanced propagation speed, and the optimization for microwave ignition sensitivity. Precursor suspensions are sonicated for 1 h for each component added and then stirred for 24 h using a magnetic stir plate/bar. The additive manufacturing technique is solvent-based and relies on the evaporation of DMF, which was aided by maintaining the print bed at 70 °C. The drying process is controlled by the temperature of the printing bed, the speed and extrusion rate of the print, and solvent exhaust venting. Dry times were on the order of 15–30 s after deposition with the resulting four-layer film thickness being 30–40 μm (7–10 μm/layer) as shown in Fig. S3 in the supplementary material. A minimum of four layers of printed material are required to effectively remove the samples from the printing surface. Films for flame speed and ignition tests are printed in rectangular sheets from which multiple free-standing thin strands (1 mm × 2 cm) may be harvested. More complex architectures are printed using multiple printing codes designated for specific formulations, which work in tandem to complete the final multicomponent architecture. Multicomponent architecture prints have layers of different formulations printed directly on top of a previous layer in a partial-layering scheme. Figure S3 in the supplementary material depicts cross section images of Al/PVDF and Ti/PVDF samples printed with four layers at ∼8 μm/layer.

D. Burn rate characterization

Combustion performance of printed energetics was evaluated using 1 mm-wide energetic strands that were cut from larger printed sheets and burned in a controlled atmosphere. As shown in Fig. S4 in the supplementary material, the strands are loaded into a glass cylinder closed off with rubber stoppers that have gas inlets and electrodes. The strands are mounted between two braided nichrome wires and anchored at the opposite end with double-sided tape. Strands are ignited by resistively heating the nichrome wire and the combustion event was recorded using a high-speed camera (Phantom Miro M110) recording at 10 000 frames/s. The burn rate is calculated by tracking the pixel coordinates of the flame front as a function of time and considering the pixel/distance ratio determined from the precisely spaced metal plates in the foreground of the video.

Burn rate experiments for all samples were performed in both air and argon environments to reduce the dependence of oxygen on the observed ignition and propagation characteristics. Anaerobic combustion tests used argon (Airgas 99%) to purge the glass tube for ∼5 min followed by the simultaneous closure of the inlet/outlet prior to the ignition event.

E. Focused microwave ignition

To precisely localize the ignition of the microwave-sensitive energetic composites, a needle-based, coaxial microwave emitter was designed and suspended over the printed films.[23] A critical characteristic of this design is the ability to concentrate microwave energy into an area much smaller than the chosen wavelength. In this configuration, a solid-state power amplifier (AMCOM AM206545SF-3H) with a peak gain of 32 dB drives a 2.45 GHz, 10 dBm continuous wave tone from a microwave signal generator (DS Instruments SG12000). This brings the peak power output of the device to approximately 42 dBm, or 15 W (see Fig. 1). A coaxial-solder pin adapter was soldered to a nickel-plated straight pin (Singer 0.025 in. diameter). The printed film sample sits on a glass slide, and the slide is positioned over a grounded surface. A simulation of the electric fields through Ansys HFSS illustrates that the field intensity (∼100 kV/m) is most concentrated between the pin and ground plane with the sample in its path. This field is an order of magnitude lower than the dielectric breakdown point of air at 1 atm (∼3000 kV/m) and does not result in electrostatic discharge (ESD) events.

Since the working distance from the emitter to the sample is much smaller than the operating wavelength, sample exposure is in the "near-field" of the electromagnetic (EM) field, implying there will be some coupling between the sample and the antenna. Concentrating microwave radiation in the far-field down to a point would require a large antenna design and sample size but would result in the same phenomenon and observations presented here.

Combustion events of the needle-based microwave ignition experiments were observed using a high-speed camera (Phantom Miro M110), which was triggered simultaneously with the power input to the microwave amplifier.

Samples tested in argon with the microwave needle assembly were placed inside a glass tube with gas inlets. A small sample of the material was placed inside the tube, the tube was purged with argon, and the needle was then placed through an opening in the tube to access the interior for sample heating. Videos recorded used the same high-speed camera as was used in the other experiments described.

III. RESULTS AND DISCUSSION

A. Microwave absorption of metals and material selection

Efficiency of microwave heating is closely related to material properties such as electrical conductivity (σ), permittivity (ε), and permeability (μ) when interacting with electromagnetic radiation of a certain frequency (ω). As such, the total averaged power dissipated

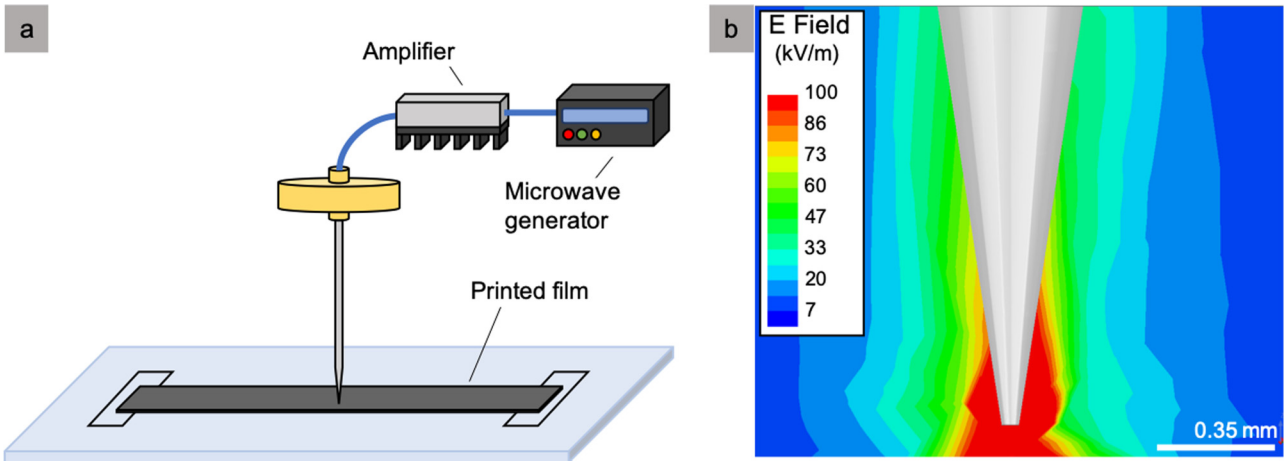

FIG. 1. (a) Needle-based microwave ignition experiment at 2.45 GHz. Peak power of the entire system is ~15 W. (b) Simulations of the electric field at the tip of the needle for a frequency of 2.45 GHz (using Ansys HFSS and an auto-generated mesh).

(P_d) within a material is linked to these properties in their ability to couple with the electric field (E) and magnetic field (H) of the incident electromagnetic radiation. A steady-state electromagnetic energy balance between the energy flux delivered by the microwave to the surface of the material, described by the Poynting vector, and the time averaged energy dissipated per unit volume yield Eq. (1).[18,27] The permittivity, $\varepsilon = \varepsilon_o(\varepsilon_r' - j\varepsilon_r'')$, and permeability, $\mu = \mu_o(\mu_r' - j\mu_r'')$, are generally complex with the real parts representing a measure of energy storage from the EM wave within the material and the imaginary part representing the energy dissipated within the material,[17]

$$P_d = \frac{1}{2}\sigma|E|^2 + \frac{1}{2}\omega\varepsilon_o\varepsilon_r''|E|^2 + \frac{1}{2}\omega\mu_o\mu_r''|H|^2. \quad (1)$$

Each term on the right side of Eq. (1) represents, from left to right, the conduction, dielectric, and magnetic heat losses, respectively, where the solution to the electric and magnetic field throughout the volume of the material may be solved by using the Maxwell equations for materials.[18,27] The general form of this solution is a traveling plane wave with an exponential attenuation factor to represent the loss of energy of the incident radiation. The characteristic attenuation factor is related to what is colloquially known as the skin depth of a material and represents the length scale to which incident electromagnetic radiation may penetrate a material to efficiently heat.[18,20,27] The skin depth is dependent on the frequency of the incident electromagnetic radiation and the electrical conductivity of the material. Metals generally have a skin depth on the order of a few micrometers where the optimal size of particles for absorption of microwave energy is of the same order of magnitude as the skin depth.[20,21] Based on this information, and the previous findings mentioned in the Introduction, working with nanometals should be intrinsically difficult given that nanoparticles have diameters that are 100 times smaller than the skin depth.

Having set the candidate criteria (as discussed in Sec. II), we began by studying the most-widely used metal fuel—aluminum. Aluminum-based energetics are well-studied in the literature and incorporation into a polymer [particularly poly(vinylidene fluoride), PVDF] has proven successful in making solid propellants that can be readily manufactured.[4,5] Unfortunately, our initial investigations into microwave heating of Al proved unsuccessful, which led us to consider using a reactive metal as an initiator for aluminum-based composites. As this paper will demonstrate, titanium nanoparticles and titanium-based composites proved to be highly successful at igniting via microwave exposure. The reasons for its effectiveness are discussed below.

A comparison of microwave power absorption by ensembles of aluminum and titanium nanoparticles in an inert medium was conducted using the Mie theory.[27,28] The intensity fraction absorbed is given by Eq. (2) where I_{abs} is the absorbed intensity, I_0 is the incident intensity, σ_A is the absorption cross section, N is the number density of particles, and d is the path length (as characterized by the layer).[31]

$$\frac{I_{abs}}{I_0} = 1 - e^{-\sigma_A N d}. \quad (2)$$

Equation (2) is derived from the Beer–Lambert law, which is a valid assumption since the scattered radiation is small given that the particle size is much smaller than the wavelength of light and the scattered radiation from other particles would not interact. The effective relative complex permittivity for Ti and Al were estimated using the Drude model approximation for metals $\left(\tilde{\varepsilon}_r \approx \tilde{\varepsilon}'_r + j\frac{\sigma}{\omega\varepsilon_o}\right)$.[18,27,32] For an operating frequency of 2.45 GHz, the approximate effective relative permittivity of highly conductive particles is dominated by the imaginary loss term, $\tilde{\varepsilon}_r''$, which in this model is directly related to electrical conductivity and Joule heating terms in Eq. (1).[21,32] Finally, since both metals are nonmagnetic, the magnetic permeability for all materials is assumed to be 1. Calculated values for all aforementioned constants can be seen in Table S1 in the supplementary material.[17,21,33,34]

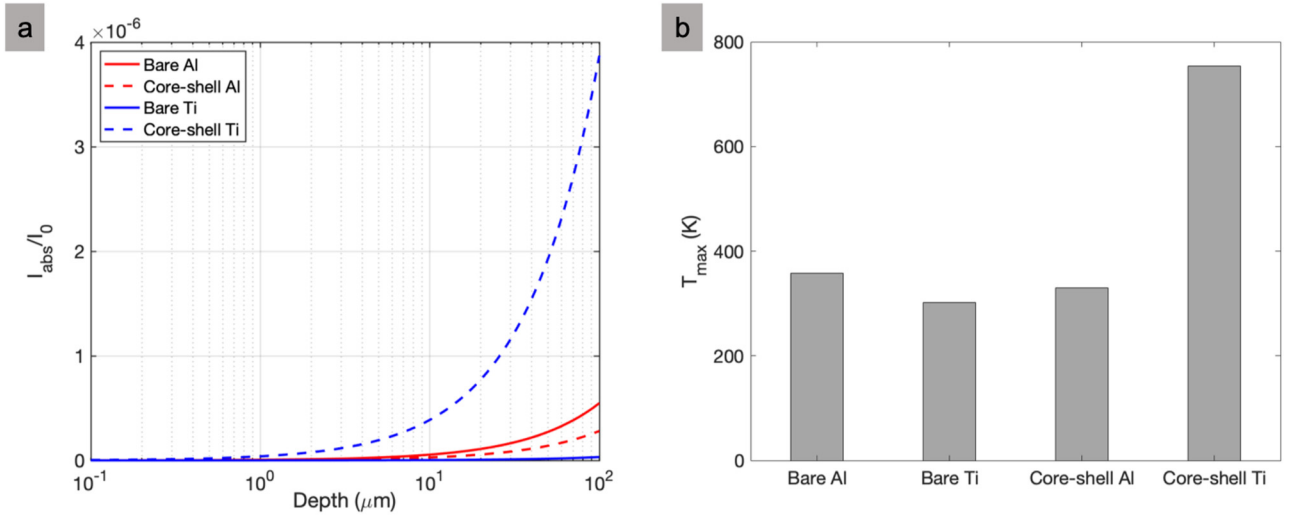

FIG. 2. (a) Calculated fraction of microwave (2.45 GHz) intensity absorbed for bare and core–shell Al and Ti nanoparticles in a 25 μm diameter cylinder as a function of depth and (b) the estimated maximum temperature after being exposed to a microwave input of 15 W for 0.5 s. Physical properties used in calculation are provided in Table S1 in the supplementary material.

Figure 2(a) shows the resulting Mie theory fractional microwave extinction as a function of layer thickness of a composite comprised of 80 nm metal particles. Most interesting is that, even though as-received core–shell nTi is an effective absorber relative to core–shell Al in the experiment (discussed in Sec. III B), the Mie calculation indicates otherwise for bare particles. When one considers nanoparticles, a nontrivial fraction of the mass is concentrated in the passivating shell. The shell composition of core–shell nanoparticles may be characterized by a combination of x-ray photoelectron spectroscopy (XPS) and x-ray diffraction (XRD). Aluminum naturally forms a 2–10 nm passivating oxide (Al_2O_3) shell that can dramatically impact combustion performance and material properties at small particle sizes.[35,36] Titanium nanoparticles readily acquire a shell of similar thickness, but instead demonstrate, from XPS, mixed molar compositions of TiN (~20% by number) and TiO_2 (~80% by number) when exposed to air.[2] Considering this difference in the shell composition, previous studies regarding the microwave sensitivity of metals by other groups may have failed to consider the impact that the passivating shell may have on the interaction of the electromagnetic field with the internal pure metal content.[20]

Figure 2(a) shows the calculated absorbed microwave (2.45 GHz) intensity for the passivated Al and Ti nanoparticles where the inclusion of the shell significantly impacts the estimated absorbed intensity. Although bare Al nanoparticles are expected to absorb more power than similarly sized Ti particles, the inclusion of nTi passivating shell increases the intensity absorbed by an order of magnitude over the Al equivalent. This suggests that the shell must play a significant role in the heating of metal particles. The transparency of Al_2O_3 does not enhance the absorbed fraction of the metal nanoparticles,[17] while the material properties of TiN and TiO_2 increase the power fraction absorbed of the otherwise inferior microwave absorbing bare Ti particles.[28]

The material properties alone do not explain why aluminum nanoparticles are so drastically inefficient at coupling with microwaves compared to Ti nanoparticles since both particle types are exposed to the same method of heating. Models considering bare metal particles suggest that heating is dominated by induced eddy currents from the magnetic field.[20,21] However, even micrometer sized aluminum particles cannot be efficiently heated. As particles are reduced to the nanoscale, the magnetic contribution drastically diminishes, further ruling out any significant heating from microwave absorption. Concurrent work by our research group expanding the system to a core–shell system has shown, from the Mie theory approach, that the behavior of the previous models is recaptured. Additionally, this model shows that the core–shell structure at these length scales, in combination with the material properties of the core–shell, can significantly enhance the dissipation of power through the electric field of the microwave to several orders of magnitude higher than the magnetic field contribution when at its peak.[28]

The maximum achievable temperature of the coated and bare metal particles was estimated using the calculated power fraction absorbed, the thermophysical properties of the contents (heat capacities retrieved from the NIST WebBook and averaged over the core–shell system on a mass basis), and assuming a power input of 15 W for 0.5 s over a circular area with a ~25 μm diameter. The particles are assumed to be perfectly insulated with volumetric heating throughout the entire particle, therefore these results would represent the upper bound of the temperature reach over the 0.5 s heating interval. When accounting for the passivating shell on the Ti and Al particles, the added power absorption contribution by the Ti shell increases the estimated temperature to ~750 K-above the documented ignition temperature of Ti in air (~670 K).[2] The increased power transmission provides more efficient heating of the higher energy density Ti core, leading to thermal ignition.

B. Microwave sensitivity of metal powders

Potential nanopowder fuels for solid propellant precursor materials were tested in air for sensitivity to microwaves by first observing whether the bare powder would absorb enough microwave energy to be heated to sufficiently high temperatures for ignition. Consistent with the previous literature, aluminum particles were unable to be sufficiently heated with microwaves, independent of the particle size.[19] Aluminum particle sizes ranging from 80 nm–14 μm were unable to ignite with microwave energy, reaffirming the poor coupling to the sample and potential hindrance by the oxide shell of Al_2O_3.[37] In contrast to the results for the aluminum particles, titanium nanoparticles subject to the microwave needle assembly demonstrated heating phenomena within several milliseconds of the microwave amplifier being powered (see Fig. 3). The heating event appears to originate from a single location that is approximately near the location of the maximum electromagnetic field. The heat is quickly transferred to the surrounding particles from this hotspot as the Ti begins reacting with the O_2 in air until the sample is uniformly heated. One important consideration in these experiments would be the impact of electrostatic discharge (ESD) (arcing) within the spacing between the particles that could transfer enough energy to start the reaction.[14] However, no visible anisotropic discharge events were identifiable for any of the samples tested during the ignition process.

Microwave heating of Ti nanoparticles was also performed in an inert atmosphere in order to demonstrate heating without reactive heat generation. This was done using the microwave needle assembly which was placed into an argon environment using a glass tube with gas inlets and a small opening at the top for microwave needle access. Upon powering the microwave amplifier, the metal powders immediately surrounding the antenna began to heat to glowing temperatures within milliseconds. However, unlike the experiments performed in air, the particles would continually glow without the heat being transferred to nearby particles due to the lack of O_2 and N_2, preventing the exothermic formation of TiO_2 or TiN (see Fig. S5 in the supplementary material). These results demonstrate that not only can Ti nanoparticles be heated to high temperatures using microwaves, but also the high temperatures achieved are not solely dependent on the Ti reaction with air. The heating of Ti nanoparticles in air merely enhances the heat generation for thermal propagation away from the localized microwave source through its strongly exothermic reaction with air. The sensitivity of the Ti particles to microwaves further alludes to the importance of shell composition on particle heating. Experimentally, core–shell Ti nanoparticles can couple to microwaves more efficiently, thus heating faster and ultimately achieve thermal ignition as opposed to core–shell Al nanoparticles that are unable to be heated via this method.

As mentioned previously, the observed heating and ignition of the samples by microwaves is likely attributed to (1) the unique shell composition of the Ti nanoparticles and (2) the lower ignition temperature of Ti particles in air. Electrical conductivities of materials found in the nano-Ti shell (TiN, TiO_2), while having a wide range of reported values depending on the crystal structure and physical architecture, are consistently larger than those for the Al_2O_3 found on the exterior of the Al nanoparticles.[17,21,33,34] Microwaves couple well with Ti nanoparticles as a result of unique material properties and its core–shell structure. The entire particle is heated via Joule

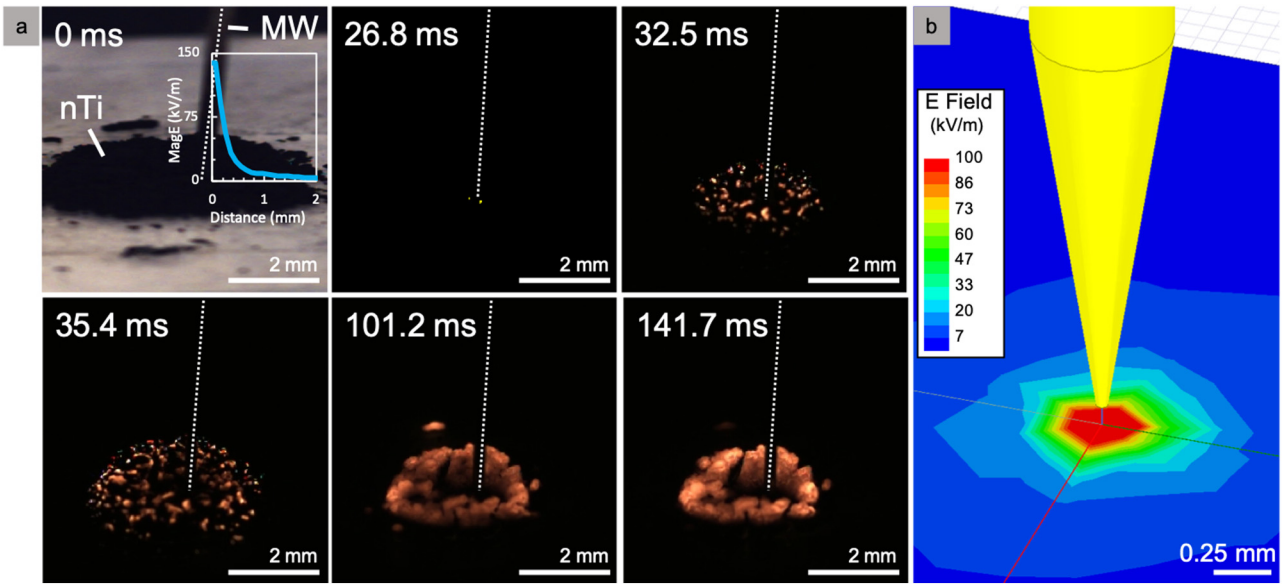

FIG. 3. (a) Ignition of nano-Ti powder in air (50 nm diameter) using microwave needle apparatus imaged using a high-speed camera. t = 0 is defined as starting time for power supplied to the applicator. The dashed white line indicates the position of the needle. (b) Simulation of the experiments in (a) showing the near-field electric field on the ground plane performed using Ansys HFSS and an auto-generated mesh.

heating originating from the dynamic nature of electromagnetic waves, resulting in frictional heat caused by induced eddy currents and shell enhanced induced polarization from the magnetic and electric components of the microwave, respectively.[20,21,28]

C. Microwave sensitivity of metallized propellants

While we have demonstrated the potential to ignite Ti-based energetic materials remotely using microwaves, the applications of the mixtures tested thus far are limited in scope. Pure metal powders react rather slowly despite their high energy density. One particularly interesting application of remote ignition would be solid propellant mixtures since they have received renewed interest with the rise of additive manufacturing.[6–8,38,39] By incorporating metal particles into an energetic polymer solution, solid propellants can be easily manufactured by additive manufacturing technologies with tailorable architectures to produce custom performances based on their physiochemical properties.

Solid energetic precursors of Ti/PVDF were prepared with varying weight percentages of Ti, as shown in Table I, to investigate the role of Ti metal particles on ignition. It was expected that the addition of PVDF to the Ti particles would impact the ignition of the materials, especially considering that particles would be predominately encapsulated in the polymer throughout the film. It was observed that at an equivalence ratio (Φ) of 1, Ti (35 wt. %)/PVDF (65 wt. %) will not be ignited by microwave radiation, but increasingly Ti fuel rich compositions will ignite more readily and consistently. Ti (50 wt. %)/PVDF (50 wt. %) was found to be a lower bound for microwave ignitability for which heating was inconsistent at times. Additionally, the level of Ti particle inclusion must also be balanced with printability where Ti (65 wt. %)/PVDF (35 wt. %) was found to be the upper bound for Ti loading. A summary of these results is presented in Table II. An important note is that electrical percolation may be contributing to the microwave sensitivity of these composite propellants; however, all results and calculations presented thus far suggest that the as-received Ti nanoparticles would ignite irrespective of percolation.[40] A detailed analysis on percolation thresholds is beyond the scope of this article but should be considered in future research.

When tested with the needle-based microwave applicator, Ti/PVDF samples containing 65 wt. % Ti were readily ignited within 10 ms of power being delivered to the samples with the propellant films consistently propagating to completion in air (see Fig. 4) and argon (discussed in Sec. III D). Upon ignition of the sample, a bright ignition point becomes clear with particles being ejected from the surface shortly after. Within 65 ms, a uniquely shaped circular reaction front with an approximate width of ~0.3 mm began propagating from the hotspot until it reached the edge of the film at which point the propagation became linear. The flame structure of the Ti/PVDF films during combustion strongly resembles those that are seen in Al/PVDF combustion events with a long, hot reaction tail, which generates a significant amount of soot; however, a detailed study is reserved for future research. While the structure of the flame will be explored in future work, the bidirectional and steady propagation of the Ti/PVDF film opens up unique avenues by which to employ this material as a remote ignition source with high targetability.

TABLE II. Free-standing burn velocities in air and argon environments and the ability to be ignited with microwaves.

Sample	Metal wt. %	Environment	Burn velocity (cm/s)	MW ignition
Al/PVDF	25	Air	~14 ± 1	N
		Argon	~7 ± 1	N
	65	Air	~27 ± 2s	N
		Argon	~15 ± 4	N
Ti/PVDF	35	Air	~1 ± 0.5	N
		Argon	…	N
	65	Air	~4 ± 0.1	Y
		Argon	~1 ± 0.1	Y

D. Controlled-environment combustion characteristics of metallized propellants

Flame speed experiments of Al/PVDF and Ti/PVDF were performed in air and argon environments to evaluate the potential for implementation into a solid propellant. Al/PVDF has been previously investigated as an additively manufactured solid propellant; however, Ti/PVDF has yet to be fully studied.[5,29,30] While air would likely be the environment for combustion of these materials, argon was also considered to study flame self-propagation performance within an environment devoid of both oxygen and nitrogen.

Results of the average burn velocity of four samples of Al/PVDF and Ti/PVDF at different mass loadings of metal fuel are presented in Table II where it can be seen that the burn velocity of Al/PVDF samples consistently outperforms the Ti/PVDF equivalents (raw data in Figs. S6–S9 in the supplementary material). While the inert argon environments do substantially impact the burn velocities of both sample types, Al/PVDF is still able to burn at faster rates with lower metal loadings than Ti/PVDF did in air. Furthermore, low-Ti-content energetic samples were unable to sustain combustion in the inert environment. It is believed that the kinetics of the Ti/PVDF reaction in an Ar environment are not favorable since XRD analysis of postcombustion products predominately show TiF_3 as the primary product (see Fig. S10 in the supplementary material), whereas one would expect the formation of TiF_4, indicating that the reaction is not going to completion. In contrast, when the Ti/PVDF samples are burned in air, the Ti also exothermically reacts with O_2, which would assist in any shortcomings in the energy release due to incomplete reactions with PVDF.

From these results, one can see that while both Al/PVDF and Ti/PVDF samples can propagate in both air and argon environments, the Al/PVDF samples would be more desirable as a conventional solid propellant since it would be able to generate more thrust by releasing similar amounts of stored energy over shorter periods of time. However, the insensitivity of aluminum to ignition by microwave radiation limits the ability of the propellant to be utilized in remote-initiation situations. Considering the limitations between the propellant formulations, it would be desirable to have a microwave-sensitive propellant that does not have reduced performance. A potential architecture is explored in Sec. III E.

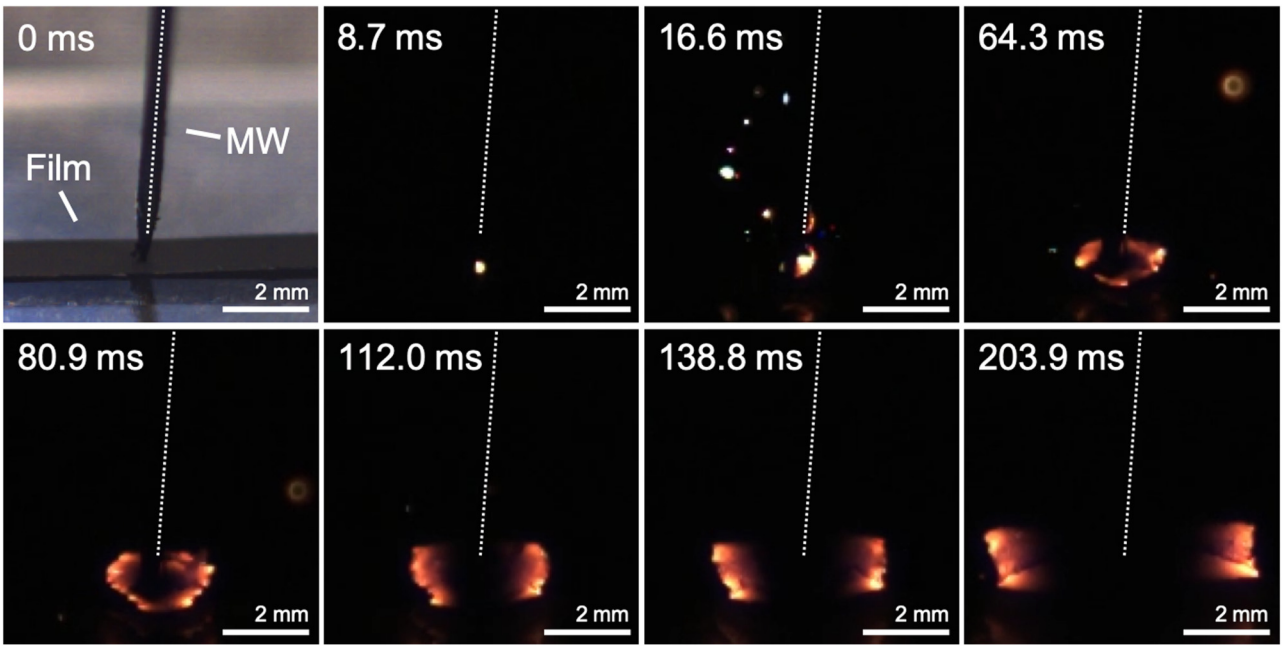

FIG. 4. Ignition of Ti/PVDF (65 wt. % Ti) film in air using microwave needle apparatus imaged using a high-speed camera. t = 0 is defined as starting time for power supplied to the applicator. The dashed white line indicates the position of the needle.

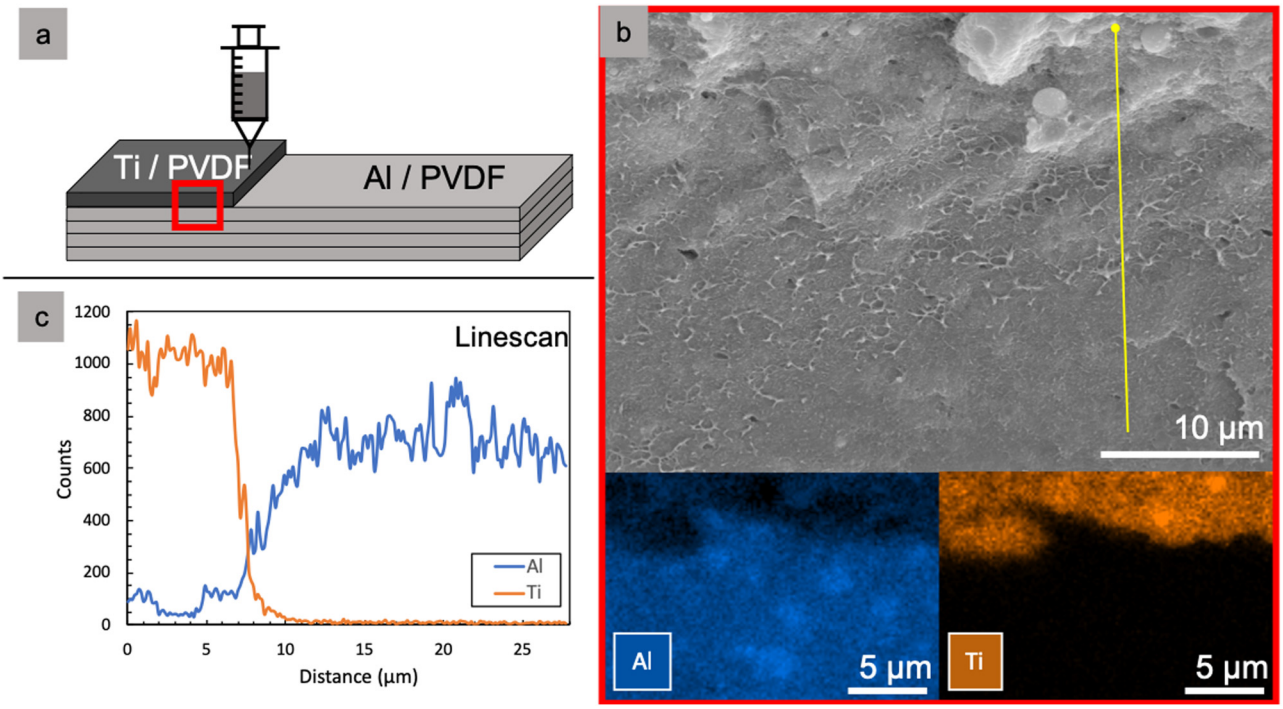

FIG. 5. (a) Depiction of the architecture for a layered Al/PVDF, Ti/PVDF propellant that can be initiated with microwaves where layers 1–4 are Al/PVDF ($\Phi = 1$) and layer 5 is Ti/PVDF (65 wt. % Ti) ($\sim 35\,\mu$m thick). (b) SEM/EDS image of the layered film cross section as outlined in (a). (c) EDS line scan results for the line drawn in (b).

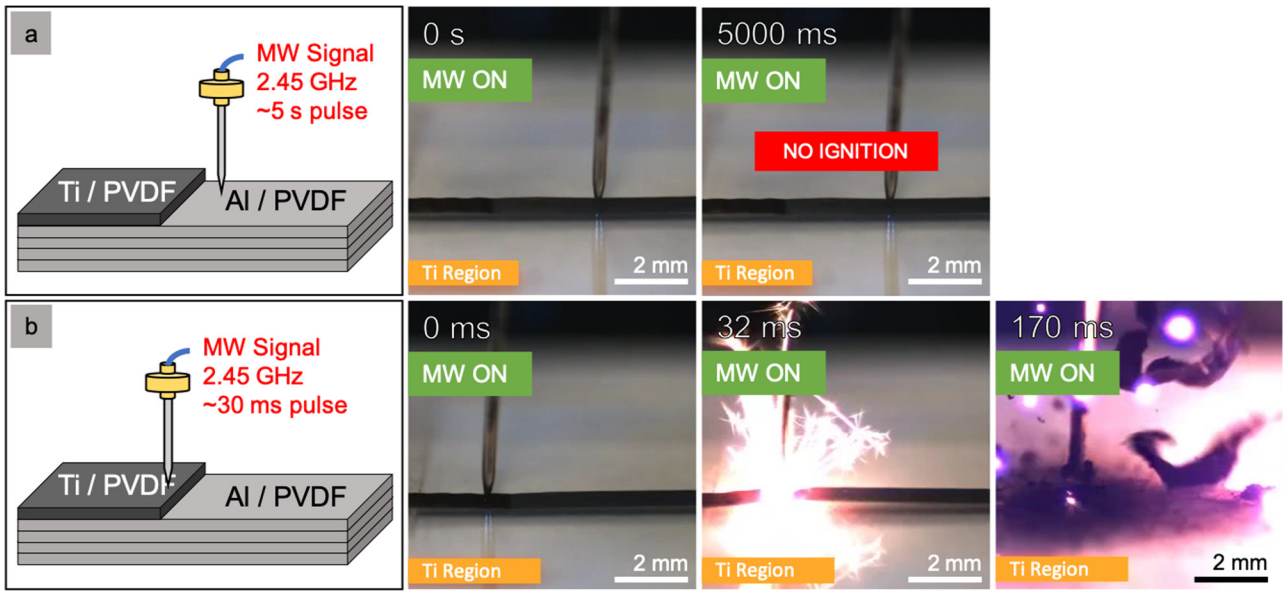

FIG. 6. Microwave needle ignition of a layered Al/PVDF, Ti/PVDF propellant where layers 1–4 are Al/PVDF ($\Phi = 1$) and layer 5 is Ti/PVDF (65 wt. % Ti). (a) Al/PVDF region does not ignite when exposed to microwave radiation and (b) Ti/PVDF layered region ignites and propagates into Al/PVDF region.

E. Architecturing of a microwave-initiated solid propellant

The results presented thus far in this work suggest that, while Ti/PVDF may not be an optimal solid propellant choice with a slow propagation velocity, it can be readily ignited in both aerobic and inert environments using targeted microwave radiation and will steadily propagate in these environments at high mass loadings of Ti. Although Al/PVDF does not have the same microwave sensitivity, its relatively superior combustion performance as a propellant and relatively low manufacturing cost still would likely steer most rocketeers toward using Al/PVDF (or some other aluminum-based metallized composite) as a primary propellant mixture.[5,41–44] As such, this work also investigated the potential incorporation of Ti/PVDF in an igniter application for Al/PVDF propellants that are additively manufactured.

An Al/PVDF precursor ($\Phi = 1$) was prepared and printed four-layers high (~30 μm) using a direct-write additive manufacturing method. A Ti (65 wt. %)/PVDF (35 wt. %) layer was then printed in a smaller segment on top of the Al/PVDF sample. A depiction of the sample can be seen in Fig. 5 and scanning electron microscopy/energy-dispersive x-ray spectroscopy (SEM/EDS) images demonstrate a clear separation between the Al/PVDF and Ti/PVDF layers that were printed. A line scan of the sample originating from the Ti/PVDF sample shows that the single Ti/PVDF layer is ~7 μm thick and that the Al/PVDF section is ~4× thicker than the Ti/PVDF domain with a total thickness of roughly 35 μm.

Combustion experiments were performed using the needle-based apparatus in aerobic and inert environments, which yielded positive results for Ti/PVDF to act as a microwave-sensitive ignition source for Al/PVDF. Figure 6 shows that the microwave sensitized Ti/PVDF layer printed on top of the larger Al/PVDF strand can be ignited ~30 ms after power is supplied to the microwave needle. Within 20 ms after the Ti/PVDF ignition, the exothermic reaction then transfers enough heat to the underlying Al/PVDF layers to rapidly (<1 ms) reach its ignition temperature of ~620 °C, leading to sustained propagation.[30] Figure 5 and Video 1 in the supplementary material also demonstrate how the ignition location can be selectively placed over a microwave-insensitive Al/PVDF layer and captures the reaction propagation transition from the Ti/PVDF into the Al/PVDF.

By making a specific segment of solid propellant remotely initiated using selectively placed microwave-sensitive materials, this work sets up the development of remotely staged, additively manufactured solid propellants. Currently, solid rocket motors do not have an "off" switch like their liquid rocket engine counterparts. Incorporating a small, inert "quenching" region with low thermal conductivity into a solid rocket motor assembly, followed by another microwave-sensitive ignition source, could provide "checkpoints" between different stages of the rocket and even a moderate throttle control (multiple segments simultaneously) using only a directional microwave radiation source and an antenna. The design of the solid propellant could be readily implemented using more sophisticated additive manufacturing techniques and would significantly improve the versatility of solid rocket motors for civilian and military applications.

IV. CONCLUSIONS

This work investigated the localized ignition of metal powders and metallized 3D printed propellants via microwaves. Materials were subjected to microwaves via a needle applicator, which was

able to ignite titanium nanopowders and energetic composites containing high mass loadings of Ti (~65 wt. %). Aluminum powders and Al/PVDF propellants were unable to be heated with the needle applicator after 30 s of exposure. Titanium's observed interaction with microwave radiation is unexpected from the point of view of models which focus on bare metallic nanoparticle–microwave coupling with no consideration of the native oxide layer composition. These observations reveal the necessity of rigorous models that consider the properties and role of the oxide layer of energetic metallic nanoparticles in microwave heating. Despite the superior microwave absorption of nanoscale titanium, the superior burn velocity and reduced cost of Al/PVDF make it a more attractive propellant for traditional propulsion applications. The Ti/PVDF composite proved to be a suitable microwave-based igniter for solid propellants in both aerobic and inert environments. This work sets the stage for studies that focus on the shell composition for enhanced microwave coupling of heterogeneous energetic systems as well as for highly tailorable combustion of solid rocket propellants that can be remotely ignited and staged with directed microwave radiation.

SUPPLEMENTARY MATERIAL

The online supplementary material for this article includes a schematic of the macroscopic burn test apparatus, physical constants used in microwave absorption calculations, electron microscopy images of printed films, images from Ti heating in an argon environment, raw data for propagation velocity tests, and postcombustion product analysis.

AUTHOR'S CONTRIBUTIONS

D. J. Kline and M. C. Rehwoldt contributed equally to this work.

ACKNOWLEDGMENTS

The authors gratefully acknowledge the support from the U.S. Air Force Office of Scientific Research (AFOSR). Electron microscopy was performed with the NNS450 Scanning Electron Microscope at the Central Facility for Advanced Microscopy and Microanalysis (CFAMM) at the University of California, Riverside. We would also like to acknowledge Dr. Brian Beaudoin at the University of Maryland Institute for Research in Electronics and Applied Physics (IREAP).

REFERENCES

[1]J. B. DeLisio, X. Wang, T. Wu, G. C. Egan, R. J. Jacob, and M. R. Zachariah, J. Appl. Phys. **122**, 245901 (2017).
[2]M. C. Rehwoldt, Y. Yang, H. Wang, S. Holdren, and M. R. Zachariah, J. Phys. Chem. C **122**, 10792 (2018).
[3]Y. Chen, D. R. Guildenbecher, K. N. G. Hoffmeister, M. A. Cooper, H. L. Stauffacher, M. S. Oliver, and E. B. Washburn, Combust. Flame **182**, 225 (2017).
[4]C. Huang, G. Jian, J. B. De Lisio, H. Wang, and M. R. Zachariah, Adv. Eng. Mater. **17**, 95 (2015).
[5]H. Wang, M. Rehwoldt, D. J. Kline, T. Wu, P. Wang, and M. R. Zachariah, Combust. Flame **201**, 181 (2019).
[6]T. J. Fleck, A. K. Murray, I. E. Gunduz, S. F. Son, G. T.-C. Chiu, and J. F. Rhoads, Addit. Manuf. **17**, 176 (2017).
[7]M. S. McClain, I. E. Gunduz, and S. F. Son, Proc. Combust. Inst. **37**, 3135 (2019).
[8]S. C. Ligon, R. Liska, J. Stampfl, M. Gurr, and R. Mülhaupt, Chem. Rev. **117**, 10212 (2017).
[9]S. J. Barkley, K. Zhu, J. B. Michael, and T. R. Sippel, in *AIAA Scitech 2019 Forum* (American Institute of Aeronautics and Astronautics, 2019).
[10]T. Sippel, "Pulsed microwave plasma instrumentation for investigation of plasma-tuned multiphase combustion," Final Report, DISTRIBUTION A: Distribution Approved for Public Release (2018).
[11]J. D. Katz, Annu. Rev. Mater. Sci. **22**, 153 (1992).
[12]C. Leonelli, P. Veronesi, L. Denti, A. Gatto, and L. Iuliano, J. Mater. Process. Technol. **205**, 489 (2008).
[13]R. Roy, D. Agrawal, J. Cheng, and S. Gedevanishvili, Nature **399**, 668 (1999).
[14]G. M. Batanov, N. K. Bereghetskaya, V. A. Kopiev, I. A. Kossyi, A. N. Magunov, V. A. Shcherbakov, and N. V. Sachkova, Dokl. Phys. **51**, 180 (2006).
[15]S. Horikoshi and N. Serpone, *Microwaves in Nanoparticle Synthesis: Fundamentals and Applications* (John Wiley & Sons, 2013).
[16]K. Hasue, M. Tanabe, N. Watanabe, S. Nakahara, F. Okada, and A. Iwama, Propellants Explos. Pyrotech. **15**, 181 (1990).
[17]S. Horikoshi, R. F. Schiffmann, J. Fukushima, and N. Serpone, *Microwave Chemical and Materials Processing: A Tutorial* (Springer, 2017).
[18]R. Kaur, M. Newborough, and S. D. Probert, Appl. Energy **44**, 337 (1993).
[19]C. A. Crane, M. L. Pantoya, B. L. Weeks, and M. Saed, Powder Technol. **256**, 113 (2014).
[20]M. Ignatenko, M. Tanaka, and M. Sato, Jpn. J. Appl. Phys. **48**, 067001 (2009).
[21]A. Porch, D. Slocombe, and P. P. Edwards, Phys. Chem. Chem. Phys. **15**, 2757 (2013).
[22]N. Yoshikawa, E. Ishizuka, and S. Taniguchi, Mater. Trans. **47**, 898 (2006).
[23]Y. Meir and E. Jerby, Combust. Flame **159**, 2474 (2012).
[24]C. A. Crane, M. L. Pantoya, and B. L. Weeks, J. Appl. Phys. **115**, 104106 (2014).
[25]T. Kim, J. Lee, and K. H. Lee, Carbon Lett. **15**, 15 (2014).
[26]S. Chandrasekaran, T. Basak, and R. Srinivasan, Int. Commun. Heat Mass Transf. **48**, 22 (2013).
[27]C. F. Bohren and D. R. Huffman, *Absorption and Scattering of Light by Small Particles* (John Wiley & Sons, 2008).
[28]P. Biswas, G. Mulholland, M. Rehwoldt, D. J. Kline, and M. R. Zachariah, "Microwave absorption of small metal particles with different types of coatings," J. Quant. Spectrosc. Radiat. Transf. (unpublished) (2020).
[29]J. B. DeLisio, X. Hu, T. Wu, G. C. Egan, G. Young, and M. R. Zachariah, J. Phys. Chem. B **120**, 5534 (2016).
[30]M. C. Rehwoldt, H. Wang, D. J. Kline, T. Wu, N. Eckman, P. Wang, N. R. Agrawal, and M. R. Zachariah, Combust. Flame **211**, 260 (2020).
[31]D. F. Swinehart, J. Chem. Educ. **39**, 333 (1962).
[32]H. J. Kitchen, S. R. Vallance, J. L. Kennedy, N. Tapia-Ruiz, L. Carassiti, A. Harrison, A. G. Whittaker, T. D. Drysdale, S. W. Kingman, and D. H. Gregory, Chem. Rev. **114**, 1170 (2014).
[33]J. L. Rankinen, *Microwave Characterization of Thin Film Titania* (The Pennsylvania State University, 2005).
[34]C. Gong, J. Zhang, C. Yan, X. Cheng, J. Zhang, L. Yu, Z. Jin, and Z. Zhang, J. Mater. Chem. **22**, 3370 (2012).
[35]D. A. Firmansyah, K. Sullivan, K.-S. Lee, Y. H. Kim, R. Zahaf, M. R. Zachariah, and D. Lee, J. Phys. Chem. C **116**, 404 (2012).
[36]F. Noor, A. Vorozhtsov, M. Lerner, and D. Wen, Powder Technol. **282**, 19 (2015).
[37]R. K. Sharma, R. Kaneriya, S. Patel, A. Bindal, and K. C. Pargaien, Microelectron. Eng. **108**, 45 (2013).
[38]R. A. Chandru, N. Balasubramanian, C. Oommen, and B. N. Raghunandan, J. Propul. Power **34**, 1090 (2018).
[39]F. D. Ruz-Nuglo and L. J. Groven, Adv. Eng. Mater. **20**, 1700390 (2018).
[40]D. T. Zimmerman, J. D. Cardellino, K. T. Cravener, K. R. Feather, N. M. Miskovsky, and G. J. Weisel, Appl. Phys. Lett. **93**, 214103 (2008).

[41]H. Wang, J. Shen, D. J. Kline, N. Eckman, N. R. Agrawal, T. Wu, P. Wang, and M. R. Zachariah, Adv. Mater. **31**, 1806575 (2019).
[42]H. Wang, J. B. DeLisio, S. Holdren, T. Wu, Y. Yang, J. Hu, and M. R. Zachariah, Adv. Eng. Mater. **20**, 1700547 (2018).
[43]G. Young, H. Wang, and M. R. Zachariah, Propellants Explos. Pyrotech. **40**, 413 (2015).
[44]K. T. Sullivan, C. Zhu, E. B. Duoss, A. E. Gash, D. B. Kolesky, J. D. Kuntz, J. A. Lewis, and C. M. Spadaccini, Adv. Mater. **28**, 1934 (2016).